*Clinical Science* (2022) **136** 257–272
https://doi.org/10.1042/CS20210989

PORTLAND PRESS

Research Article

# Placental trophoblast-specific overexpression of chemerin induces preeclampsia-like symptoms

**Lunbo Tan[1,2,3,*], Zhilong Chen[1,2,*], Fen Sun[1,4], Zhuoqun Zhou[1,5], Baozhen Zhang[1], Baobei Wang[1], Jie Chen[1], Mengxia Li[1], Tianxia Xiao[1], Rugina I. Neuman[3], Jianmin Niu[5], Koen Verdonk[3], Xifeng Lu[6], Jian V. Zhang[1,7], A.H. Jan Danser[3], Qing Yang[2] and Xiujun Fan[1]**

[1]Center for Energy Metabolism and Reproduction, Institute of Biomedicine and Biotechnology, Shenzhen Institute of Advanced Technology, Chinese Academy of Sciences, Shenzhen, Guangdong 518055, China; [2]College of Veterinary Medicine, Hunan Agricultural University, Changsha, Hunan 410128, China; [3]Division of Vascular Medicine and Pharmacology, Department of Internal Medicine, Erasmus MC, Rotterdam, The Netherlands; [4]College of Veterinary Medicine, Shaanxi Centre of Stem Cells Engineering & Technology, Northwest A&F University, Yangling, Shaanxi 712100, China; [5]Shenzhen Maternity and Child Healthcare Hospital, Southern Medical University, Shenzhen, Guangdong 511400, China; [6]Department of Pharmacology, Shenzhen Technology University, Shenzhen 518118, China; [7]Department of Clinical Pharmacy and Translational Medicine, School of Pharmacy and Biomedicine, Shenzhen Institutes of Advanced Technology, Chinese Academy of Sciences, Shenzhen, China

**Correspondence:** Xiujun Fan (xiujun.fan@gmail.com) or Qing Yang (qingyanghn@hunau.edu.cn)



Maternal circulating levels of the adipokine chemerin are elevated in preeclampsia, but its origin and contribution to preeclampsia remain unknown. We therefore studied (1) placental chemerin expression and release in human pregnancy, and (2) the consequences of chemerin overexpression via lentivirus-mediated trophoblast-specific gene manipulation in both mice and immortalized human trophoblasts. Placental chemerin expression and release were increased in women with preeclampsia, and their circulating chemerin levels correlated positively with the soluble Fms-like tyrosine kinase-1 (sFlt-1)/placental growth factor (PlGF) ratio, a well-known biomarker of preeclampsia severity. Placental trophoblast chemerin overexpression in mice induced a preeclampsia-like syndrome, involving hypertension, proteinuria, and endotheliosis, combined with diminished trophoblast invasion, a disorganized labyrinth layer, and up-regulation of sFlt-1 and the inflammation markers nuclear factor-κB (NFκB), tumor necrosis factor (TNF)-α, and interleukin (IL)-1β. It also led to embryo resorption, while maternal serum chemerin levels correlated negatively with fetal weight in mice. Chemerin overexpression in human trophoblasts up-regulated sFlt-1, reduced vascular endothelial factor-A, and inhibited migration and invasion, as well as tube formation during co-culture with human umbilical vein endothelial cells (HUVECs). The chemokine-like receptor 1 (CMKLR1) antagonist α-NETA prevented the latter phenomenon, although it did not reverse the chemerin-induced down-regulation of the phosphoinositide 3-kinase/Akt pathway. In conclusion, up-regulation of placental chemerin synthesis disturbs normal placental development via its CMKLR1 receptor, thereby contributing to fetal growth restriction/resorption and the development of preeclampsia. Chemerin might be a novel biomarker of preeclampsia, and inhibition of the chemerin/CMKLR1 pathway is a promising novel therapeutic strategy to treat preeclampsia.

[*]These authors contributed equally to this work.

Received: 12 October 2021
Revised: 28 January 2022
Accepted: 31 January 2022

Accepted Manuscript online: 01 February 2022
Version of Record published: 14 February 2022

## Introduction

Preeclampsia is a major cause of maternal mortality, yet its pathogenesis remains unclear [1]. Preeclampsia is characterized by hypertension after 20 weeks of gestation in the presence of proteinuria or other signs of maternal organ damage such as hepatic damage [1,2].

The adipokine chemerin not only occurs in the adipocytes and liver, but also in placental trophoblasts [3,4]. It binds and activates G-protein-coupled receptor 1 (GPR1), chemokine-like receptor 1 (CMKLR1, also known as ChemR23), and CC motif chemokine receptor-like 2 (CCRL2) [5]. Its levels are elevated

*Clinical Science* (2022) **136** 257–272
https://doi.org/10.1042/CS20210989

in hypertension [3,4], diabetes [5], and non-alcoholic fatty liver disease [5]. Chemerin levels also increase during pregnancy [6,7], and since the increase is much higher in women with preeclampsia, it has been proposed that serum chemerin might be a novel preeclampsia biomarker [8,9]. Supporting its placental origin, chemerin levels fall after delivery [3,10]. Chemerin is prohypertensive and contributes to vascular remodeling [4]. It acts as a chemoattractant for immune cells and regulates angiogenesis and adipogenesis [3–5].

In the present study, we hypothesized that placental trophoblasts contribute to the elevated chemerin levels in preeclampsia and that chemerin is a determinant of preeclampsia characteristics. To explore this concept, we first quantified the placental expression and release of chemerin in healthy pregnant women and women with preeclampsia. We also compared the circulating chemerin levels with those of soluble Fms-like tyrosine kinase-1 (sFlt-1) and placental growth factor (PlGF), two well-established placenta-derived biomarkers of preeclampsia [11]. Next, we overexpressed chemerin in placental trophoblast cells by using lentivirus-mediated trophoblast-specific gene manipulation in mice, and studied its consequences in pregnancy. Finally, HTR8/SVneo cells overexpressing chemerin were used to investigate whether chemerin affects trophoblast invasion and angiogenesis.

# Methods

## Collection of blood and placental tissue from pregnant women

### Shenzhen cohort

Pregnant women receiving care at the Shenzhen Maternity and Child Healthcare Hospital were enrolled in the present study after providing written informed consent, according to a protocol that was approved by the Shenzhen Institutes of Advanced Technology, Chinese Academy of Sciences Research Board. Placentas of these women were collected immediately after delivery at the Shenzhen Maternity and Child Healthcare Hospital, Shenzhen, China. Preeclampsia was defined according to the new International Society for the Study of Hypertension in Pregnancy (ISSHP) 2018 criteria, as new-onset hypertension after 20 weeks of gestation (systolic blood pressure [SBP] $\geq$ 140 mm Hg and/or diastolic blood pressure [DBP] $\geq$ 90 mm Hg) and proteinuria ($\geq$300 mg/24 h or 1+dipstick) or other signs of maternal organ dysfunction [12]. Tissues pieces were either frozen in liquid nitrogen and stored at $-80^{\circ}$C for RNA and Western blot analysis, or fixed in 4% paraformaldehyde (PFA) in phosphate buffer and embedded in paraffin for histological analysis.

### Rotterdam cohort

This patient cohort was embedded in a previously conducted prospective cohort study in which the sFlt-1/PlGF ratio was measured in women with suspected or confirmed preeclampsia at the Erasmus Medical Center, Rotterdam between 2013 and 2016 (protocol number MEC-2013-202). The inclusion and exclusion criteria of the original study have been described before [13]. We randomly selected 29 women with confirmed preeclampsia and 30 without, based on clinical diagnosis. Preeclampsia was defined according to the ISSHP 2001 criteria as *de novo* hypertension (SBP $\geq$140 and/or DBP $\geq$ 90 mm Hg) and proteinuria (protein/creatinine ratio $\geq$30 mg/mmol or $\geq$300 mg/24 h or 2+dipstick) at or after 20 weeks of pregnancy. Superimposed preeclampsia was defined as chronic hypertension with the new onset of proteinuria or sudden increase in blood pressure or appearance of thrombocytopenia and increased liver enzymes or a sudden increase in proteinuria in patients with a preexisting proteinuria. Women who were initially suspected of preeclampsia in whom the diagnosis was not confirmed, and did not have gestational hypertension, were defined as no preeclampsia. Venous blood was taken at study entry only, and after centrifugation, serum was stored at $-80^{\circ}$C for later analysis.

## Placenta perfusion studies

Placental perfusate samples were obtained from previously conducted placental perfusion experiments in Rotterdam in which transplacental drug transfer was evaluated [14,15]. Both healthy and preeclamptic placentas were utilized. In brief, placentas were brought to the lab immediately after delivery, and after selecting an intact cotyledon, the fetal circulation (closed circuit; flow rate, 6 ml/min) was established by cannulating the chorionic artery and corresponding vein of an intact cotyledon. Maternal circulation (closed circuit; flow rate 12 ml/min) was created by placing four blunt cannulas in the intervillous space. Maternal and fetal perfusion media consisted of Krebs–Henseleit buffer at 37°C, supplemented with heparin (final concentration; 2500 IU/l) and aerated with 95% $O_2$–5% $CO_2$. In one preeclamptic placenta, sildenafil had been added to the maternal circulation at t = 0 to study transfer to the fetal circulation [14]. Samples of the maternal and fetal circulations were collected every 30 min until the end of the experiment (t = 180 min), and stored immediately at $-80^{\circ}$C. Given that acute drug addition did not affect the release of either previously studied biomarkers [16], data were analyzed irrespective of the addition of sildenafil.

## Production of lentiviral vectors

A mouse chemerin cDNA made from groin fat RNA was used to amplify the chemerin coding sequence using the following primer set: forward primer 5′-ACCGAATTCAGGTGAAGCCATGAAGTGCT-3′, with an EcoRI restriction site, and reverse primer 5′-TGCGGCCGCCTGTCTAGGGCTTATTTG-3′, with a NotI restriction site. The chemerin fragment was then cloned into the pCDH-CMV-MCS-EF1-copGFP (CD511B-1) vector (LV-GFP, System Biosciences, U.S.A.) to produce LV-mChemerin-GFP. Similarly, the human chemerin coding sequence was amplified from JEG-3 cells cDNA by using the following primer set: forward primer, 5′-TGGAAGAAACCCGAGTGCAAA-3′ and reverse primer, 5′- AGAACTTGGGTCTCTATGGGG-3′. The PCR product was ligated into the pMD18-T Vector (Takara Bio Inc., Shiga, Japan), after which the chemerin coding sequence was liberated by digestion with EcoRI and NotI and cloned into LV-GFP to produce LV-hChemerin-GFP. The constructs were transfected into packaging HEK293T cells as previously described to produce lentiviral particles [17,18], and the lentivirus-containing supernatant was harvested and tittered using the QuickTiter Lentivirus quantitation kit (Cell Biolabs Inc, San Diego, CA, U.S.A.).

## Animal studies

All animal experiments were carried out in the Shenzhen Institutes of Advanced Technology following the ARRIVE guidelines and approved by the Shenzhen Institutes of Advanced Technology, Chinese Academy of Sciences Research Board. Eight-week-old CD-1 female mice (Beijing Vital River Laboratory Animal Technology Co., Ltd., Beijing, China) were caged in a specific pathogen-free animal room with a 14-h light/10-h dark cycle, and were mated with fertile or vasectomized males of the same strain to induce pregnancy or pseudopregnancy, respectively. The day of appearance of a vaginal plug was designated as day 1 of pregnancy or pseudopregnancy (GD1). Mouse placental trophoblast-specific chemerin gene delivery was achieved by lentivirus-mediated transduction into zona-free blastocysts as previously described [17,18]. Briefly, blastocysts were flushed from the uterus on GD4, and treated with acid Tyrode's solution (Sigma–Aldrich, St. Louis, MI, U.S.A.) to remove the zona pellucidae. Individual zona-free blastocysts were incubated in 5-μl KSOM drops containing LV-GFP (Control) or LV-mChemerin-GFP (LV-mChemerin) ($2 \times 10^6$ transduction units/ml) covered with light mineral oil (Sigma–Aldrich) for 6 h. Blastocysts were then washed with M2 medium to remove excess lentiviruses and transferred to GD3 pseudopregnant mice (10–14/mouse). Fetal heart rate and embryo development status were monitored every 3 days starting from GD6 by ultrasound imaging, making use of the VisualSonics VEVO 2100 imaging system (VisualSonics, Toronto, Canada). To this end, fully anesthetized animals were placed on a 37°C heated plate [19]. The growth rate was assessed visually, on the basis of a presence of a distinctive fetal shape, i.e. a clear head and trunk feature at GD9 and GD10 by ultrasound, combined with a measurable crown-rump length at GD9, GD12 and GD15, a measurable biparietal diameter at GD9, GD12, GD15 and GD18, a measurable abdominal circumference at GD12, GD15 and GD18, a measurable placental diameter and placental thickness at GD12, GD15 and GD18, and a detectable heart rate at GD12, GD15 and GD18. The implantation rate per mother was calculated as succeeded implanted embryo number/transplanted blastocyst number. Only mice with more than four live fetuses were included in the study. SBP was measured every 3 days from GD6, as well as on post-delivery days 1 and 4 in conscious mice by a non-invasive computerized tail-cuff method (BP-2000 Visitech System; Visitech Systems Inc, Apex, NC, U.S.A.), as described previously [17]. Animals were acclimatized to the system for 1 week before use in experiments. The average BP value from ten stable consecutive measurements was calculated for each individual. Urine was collected into a polystyrene beaker at the same timepoint of different gestational days by gently tickling the mice on the back. Mice were killed by 5% isoflurane administration and cervical dislocation. Placentas, fetuses, kidneys and blood samples were collected at different gestational days. Collection was limited to well-shaped placentas (i.e., placentas characterized by a clear complete structure, including decidua, junction zone, and labyrinthine zone) and fetuses (i.e., fetuses characterized by a clear body shape, including eyes, head, apparent liver shape, heartbeat, legs, and tail), and dead fetuses and their placentas were discarded. Per litter, placentas were used for histology or mixed for the mRNA and protein analysis.

## Cell culture experiments

Immortalized human trophoblast cells (HTR8/SVneo) were donated by Dr. Charles H. Graham (Queen's University, Kingston, Canada). Human umbilical vein endothelial cells (HUVECs, three different batches) were purchased from ATCC (Manassas, VA, U.S.A.). Cells were maintained in DMEM/F12 medium (HyClone, Logan, UT, U.S.A.) supplemented with 10% fetal bovine serum (FBS) at 37°C with 5% $CO_2$. To induce chemerin overexpression, HTR8/SVneo cells were plated at a density of $5 \times 10^5$ cells/well in 96-well plates and infected with LV-hChemerin-GFP lentivirus ($2 \times 10^5$ transduction units/ml) in serum-free medium. After 24 h, the medium was replaced by fresh

*Clinical Science* (2022) **136** 257–272
https://doi.org/10.1042/CS20210989

DMEM/F12 medium supplemented with 10% FBS, and 3 days later, the medium was replaced by DMEM/F12 medium supplemented with 10% FBS and 5 μg/ml puromycin, to allow the selection of chemerin-overexpressing cells (HTR8-Chemerin cells) after 1 week. HTR8-GFP cells were generated via the same method, after infection with LV-GFP lentivirus (control group). Puromycin-selected cells were subsequently cultured in DMEM/F12 medium and exposed to either 1% DMSO (vehicle control) or 3 μmol/l 2-(α-naphthoyl)ethyl trimethylammonium iodide (α-NETA; Cayman Chemical, Ann Arbor, MI, U.S.A.) dissolved in DMSO.

### Wound healing assay

The wound healing assay has been described previously [20]. In brief, HTR8-GFP cells or HTR8-Chemerin cells were seeded in 24-well plates and cultured in DMEM/F12 medium until confluency. After 24 h of serum starvation, a central linear wound area was created by scraping the cell monolayers with a sterile 200-μl pipette tip. The wounded cell monolayers were then washed twice with Dulbecco's phosphate buffered saline (HyClone), and cultured in DMEM/F12 medium in the absence or presence of 3 μmol/l α-NETA. Five randomly chosen wound areas in each well were photographed with a CCD-BX53 camera-equipped microscope (Olympus, Tokyo, Japan) at 0, 24, and 48 h. Wound width measurement occurred by ImageJ. The speed/24 h at 24 and 48 h were calculated as (width at 0 h) − (width at 24 h), and (width at 24 h) – (width at 48 h), respectively. The n-number represents the number of different experiments that repeated this approach, with each experiment having three parallel wells per group.

### Tube formation assay

Tube formation capacity was analyzed in a Matrigel scaffold *in vitro* [21]. HUVECs plus either HTR8-GFP cells or HTR8-Chemerin cells (all at $1 \times 10^5$ cells/well) were mixed and seeded in 24-well plates (Corning, Glendale, AZ, U.S.A.) pre-coated with 8 mg/ml of Matrigel (BD Biosciences, San Jose, CA, U.S.A.) in DMEM/F12 medium supplemented with 10% FBS, in the absence or presence of 3 μmol/l α-NETA. Five randomly chosen areas in each well were photographed at 10 and 20 h. Branch length measurement and tube number quantification occurred by ImageJ. A tube was defined as a complete and closed ring structure in the field of images. Branches were defined as segments connected to junctions, with the junctions completing a tube. Branch length refers to the distance between two junctions.

### Transwell insert invasion assay

This assay has been described previously [20]. In brief, HTR8-GFP cells or HTR8-Chemerin cells were seeded into transwell inserts pre-coated with 1 mg/ml Matrigel (BD Bioscience) at $1 \times 10^5$ cells per insert in DMEM/F12 medium supplemented with 10% FBS (Matrigel:medium = 1:7). Cells on the bottom side of the inserts after 24 h were fixed with 4% polyoxymethylene and stained with 0.1% Crystal Violet. Images of cells at the lower surface were captured as described above (five randomly chosen areas/well), and the number of cells/image was determined by ImageJ.

## Biochemical measurements, Western blotting, and PCR

Human sFlt-1 and PlGF were quantified with an automated analyzer (Cobas 6000, e-module; Roche Diagnostics, Mannheim, Germany), while human chemerin was measured by ELISA (DY2324, R&D Systems, Minneapolis, MN, U.S.A.). In mice, commercial ELISAs were used to measure chemerin (MCHM00, R&D Systems), vascular endothelial growth factor (VEGF)-A (BMS619/2, eBioscience, San Diego, CA, U.S.A.), sFlt-1 (F10324-B, Shanghai Fanke, Shanghai, China), PlGF (SEKM-0124, Solarbio, Beijing, China), and albumin (E024, Beijing HYCX Bio, Beijing, China), while creatinine was measured by fluorometric assay (C011-2, Nanjing JianChen, Nanjing, China).

### Western blotting

Proteins were extracted from whole placentas by using RIPA Lysis and Extraction Buffer (Thermo Fisher Scientific, Waltham, MA, U.S.A.). Protein concentrations were determined by using the Bradford protein assay (Thermo Fisher Scientific). Twenty microgram of total protein samples were separated by SDS/PAGE and electroblotted on to PVDF membranes (Millipore, Burlington, MA, U.S.A.). Blots were blocked with 5% non-fat milk in Tris-buffered saline and incubated with primary antibodies at 4°C overnight and then with HRP-conjugated secondary antibody at room temperature for 1 h. Signals were detected and captured with the ChemiDoc MP system (Bio-Rad, Irvine, CA, U.S.A.). Bands were semi-quantified by densitometric analysis using ImageJ software. The following primary antibodies and dilutions were used: anti-chemerin (1:1000, rabbit polyclonal, Abcam, Cambridge, U.K.), anti-CMKLR1 (1:1000, rabbit polyclonal, Abcam), anti-CCRL2 (1:1000, mouse polyclonal, Abcam), anti-AKT (1:1000, rabbit monoclonal, Cell Signaling Technology, Boston, MA, U.S.A.), anti-phospho-AKT (1:1000, rabbit monoclonal, Cell Signaling Technology), anti-β-actin (1:5000, mouse monoclonal, Sigma–Aldrich), anti-PI3K (1:1000, rabbit polyclonal,

Cell Signaling Technology), anti-sFlt1 (1:1000, rabbit polyclonal, Invitrogen, Carlsbad, CA, U.S.A.), anti-VEGF-A (1:1000, rabbit polyclonal, Santa Cruz Biotechnology, Santa Cruz, CA, U.S.A.), anti-nuclear factor-κB (NFkB; 1:1000, rabbit monoclonal, Abcam), anti-matrix metalloproteinase (MMP)-2 antibody (1:1000, rabbit polyclonal, Cell Signaling Technology), anti-MMP-9 antibody (1:1000, rabbit polyclonal, Cell Signaling Technology), anti-tumor necrosis factor (TNF)-α (1:300, rabbit polyclonal, Proteintech, Wuhan, China), and anti-interleukin (IL)-1β (1:300, rabbit polyclonal, Proteintech).

### RNA extraction and real-time RT-PCR

Total RNA from mouse and human placentas was extracted using TRIzol® reagent (Invitrogen), and reverse transcription was performed with Superscript II reverse transcriptase (Invitrogen) according to manufacturer's instructions. Real-time PCR was performed using the SYBR Premix ExTaq kit SYBR Green Real-time PCR Master Mix (TOYOBO, Osaka, Japan) and the 480 Real-time PCR System (Roche, Pleasonton, CA, U.S.A.). Primer sequences are listed in Supplementary Table S1. Expression levels were determined using the comparative $C_t$ method, and β-actin was used as an internal control to normalize gene expression levels.

## Histology

Mouse placental and kidney tissue was fixed overnight at 4°C in 4% PFA and embedded in paraffin. Five-micrometer sections were used for Hematoxylin and Eosin (H&E) staining and alkaline phosphatase (ALP) histochemical staining, and 3-μm sections were used for Periodic acid–Schiff (PAS) staining. All the placental sections used for histology were taken from the center of the placentas. Each placenta section was labeled with numbers. The same sequential section of each placenta was used for the same experiment. For ALP staining, 5-μm-sections were stained with the BCIP/NBT Alkaline Phosphatase Color Development Substrate (Promega, Madison, WI, U.S.A.) according to manufacturer's instructions. For PAS staining, 3-μm-mouse kidney sections were stained with the PAS Staining kit (YEASEN, Shanghai, China) according to manufacturer's instructions. Images were captured as described above. A glomerulus that is enlarged, solidified, or swollen with endocapillary cells is recorded as a glomerulus with endotheliosis, and endotheliosis frequency was calculated by dividing the number of glomeruli with endotheliosis in one kidney section by the total number of glomeruli in this section.

Immunohistochemical (IHC) staining was performed as described previously [17], making use of deparaffinized tissue sections of human placenta (heat-treated for antigen retrieval) and frozen mouse sections fixed with 4% PFA. Sections were sequentially incubated with primary antibodies, including anti-CD 31 (1:200, rat monoclonal, BD Biosciences Pharmingen, San Diego, CA, U.S.A.), anti-cytokeratin 8 (1:100, rat monoclonal, National Institutes of Health Developmental Studies Hybridoma Bank, Iowa City, IA, U.S.A.), anti-chemerin (1:100, rabbit polyclonal, Abcam), and the corresponding secondary antibodies, i.e. donkey anti-rat IgG H&L (HRP, 1:200, Abcam), goat anti-rabbit IgG H&L (HRP, 1:200, Abcam), followed by detection with 3,3′-diaminobenzidine (TIANGEN, Beijing, China). Sections incubated with nonspecific IgG instead of a primary antibody were used as negative controls. Images were captured as described above.

Image analysis occurred in a blinded fashion by a technician, and n-numbers are provided in the Figure legends.

## Statistical analysis

Data are presented as mean ± SD or median (interquartile range). Statistical analysis was performed with GraphPad Prism (version 8, La Jolla, CA, U.S.A.). Normality of the data was assessed using the Shapiro–Wilk test. To compare two groups, the Student's *t* test or Mann–Whitney U-test (in case of non-normally distributed data) were used. For the comparison of more than two groups with one factor, Kruskal–Wallis test was applied. For the comparison of more than two groups with two factors, a two-way ANOVA was used, followed by Šidák correction for multiple testing. Pearson's correlation coefficient was calculated to assess the correlation between two variables, using prior log-transformation in case of non-normal distribution. $P<0.05$ was considered statistically significant.

# Results

## Increased placental chemerin release in preeclamptic patients

Supplementary Tables S2 and S3 provide the characteristics of the healthy and preeclamptic women whose blood samples and placentas were obtained. As expected, DBP was higher, while gestational age at delivery and birth weight were lower in the preeclamptic group. Serum chemerin levels were elevated in preeclamptic women (Supplementary Table S2), and correlated positively with the sFlt-1/PlGF ratio (Figure 1A). Chemerin release from perfused placentas

*Clinical Science* (2022) **136** 257–272
https://doi.org/10.1042/CS20210989

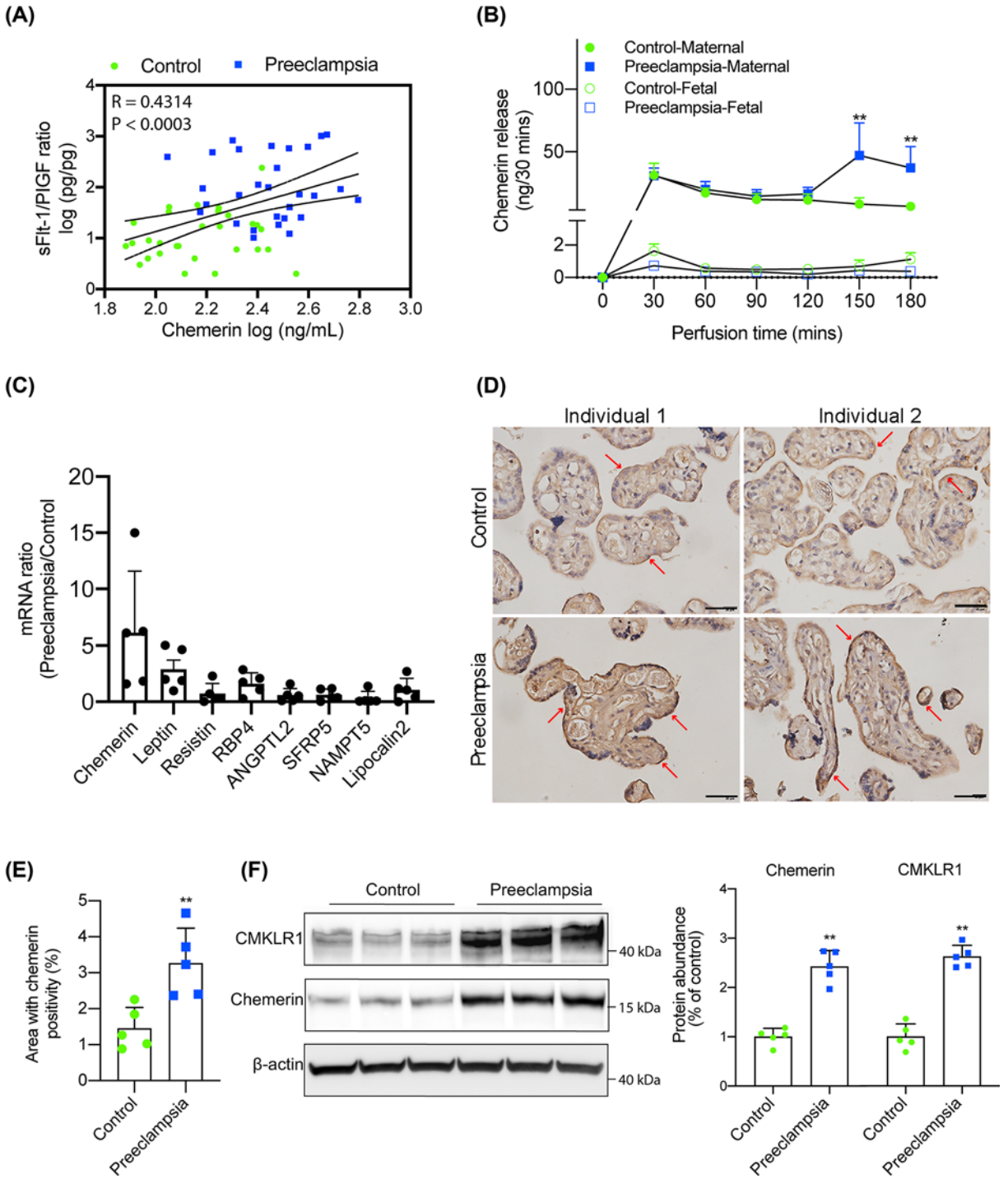


**Figure 1. Chemerin in human pregnancy**

(**A**,**B**) Relationship between chemerin and the sFlt-1/PlGF ratio in healthy pregnant (control) and preeclamptic women, and release of chemerin into the maternal and fetal perfusate during cotyledon perfusion (mean ± SD of $n$=5; $^{**}P<0.01$ by two-way ANOVA with Sidak's multiple comparisons test). (**C**) Ratio of adipocytokine mRNA levels (measured by qPCR) in placentas from preeclamptic women and healthy women (mean ± SD of $n$=5, $^{**}P<0.01$ by Kruskal–Wallis test; the mRNA ratio represents relative mRNA expression of the gene of interest in preeclamptic placental tissue divided by the average relative mRNA expression of this gene in control placenta tissue). (**D**,**E**) Representative chemerin staining in placentas (brown color, scale bar represents 50 μm), and the percentage of the area displaying chemerin positivity (mean ± SD of $n$=5; $^{**}P<0.01$ by Student's $t$ test). (**F**) Chemerin and CMKLR1 in placentas from healthy pregnant and preeclamptic women, measured by Western blotting and expressed relative to β-actin. Data are mean ± SD of $n$=5; $^{**}P<0.01$ by Student's $t$ test. (A,B) represent data from Rotterdam, all other data are from Shenzhen.

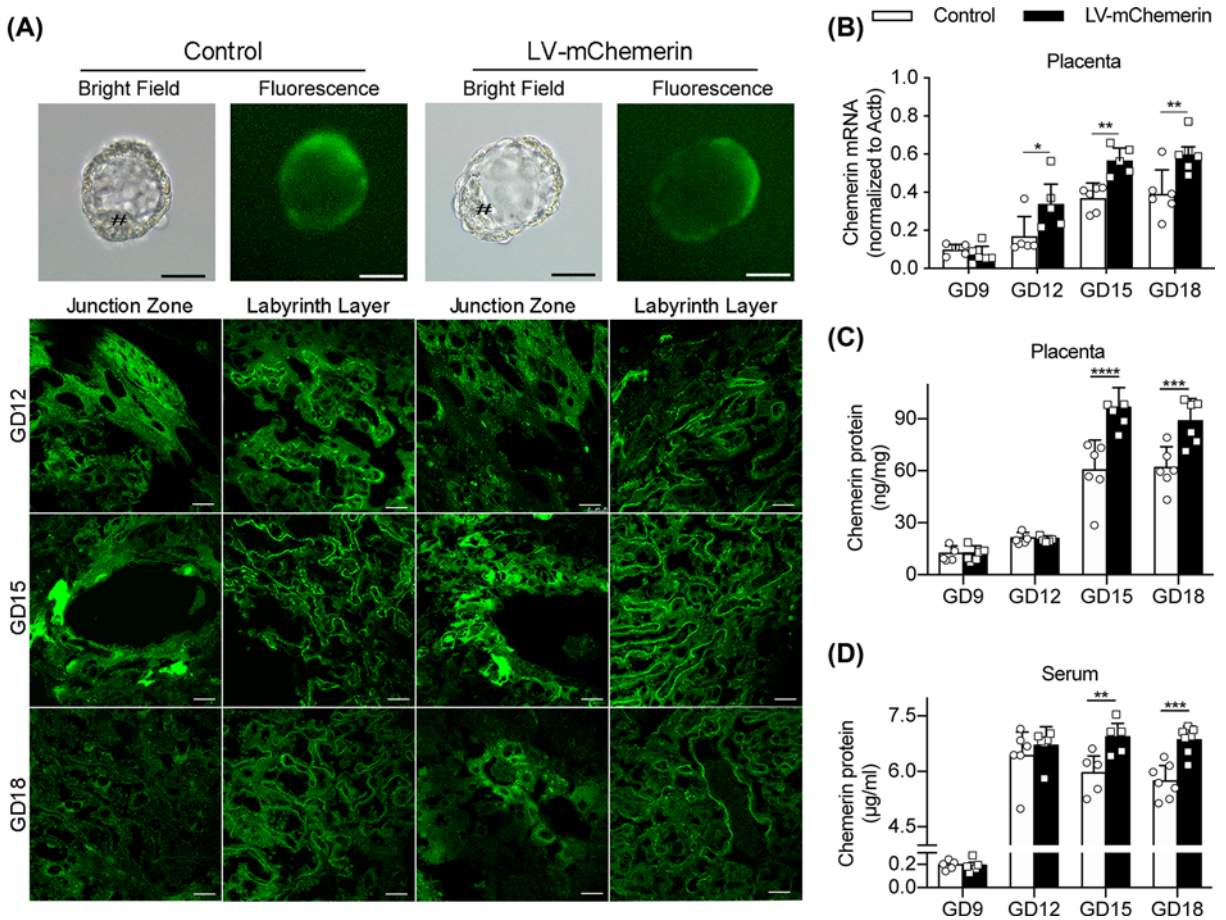


**Figure 2. Chemerin in mouse pregnancy: control mice versus mice with trophoblast-specific chemerin overexpression**

(**A**) In blastocysts transduced with lentiviruses expressing GFP alone (Control) or chemerin+GFP (LV-mChemerin), GFP is observed in the trophectoderm (denoted by #; scale bar represents 100 μm), but not the inner cell mass (four top panels), while during pregnancy GFP is expressed in the junction zones and labyrinth layers of the mouse placenta at gestational days (GD) 12, 15, and 18 (scale bar represents 25 μm). (**B–D**) Chemerin mRNA or protein levels in placenta and serum at different GD (mean ± SD of $n \geq 5$; *$P<0.05$, **$P<0.01$, ***$P<0.001$, ****$P<0.0001$ by two-way ANOVA with Sidak's multiple comparisons test).

predominantly occurred maternally (Figure 1B). The initial washout phase was identical in healthy and preeclamptic placentas. Thereafter, *de novo* release of chemerin was higher in preeclamptic placentas. In agreement with this observation, when quantifying the placental mRNA levels of adipokines, those of chemerin were elevated most in preeclampsia (Figure 1C). IHC staining (Figure 1D,E) revealed that the elevated chemerin signal in preeclamptic placentas occurred primarily in syncytiotrophoblasts. Western blotting confirmed not only the elevated chemerin levels in preeclamptic placentas, but also showed up-regulation of the chemerin receptor CMKLR1 in this condition (Figure 1F).

## Trophoblast-specific chemerin overexpression in mice

A 6-h incubation of zona-free blastocysts with lentiviral vectors expressing either GFP alone or mouse chemerin + GFP, resulted in strong GFP expression in the trophectoderm (Figure 2A). After transferring the blastocysts to day 3 pseudopregnant mice, GFP was found to be strongly expressed in the trophoblasts in the junction zone and labyrinth layer of placenta, both for the control (LV-GFP) and the LV-mChemerin groups, over several days of gestation (GD12, GD15, and GD18; Figure 2A). The chemerin mRNA levels in the LV-mChemerin group were increased at GD12, GD15, and GD18 (Figure 2B). Also, chemerin protein levels in placenta (Figure 2C) and serum (Figure 2D) were significantly increased at GD15 and GD18.

*Clinical Science* (2022) **136** 257–272
https://doi.org/10.1042/CS20210989

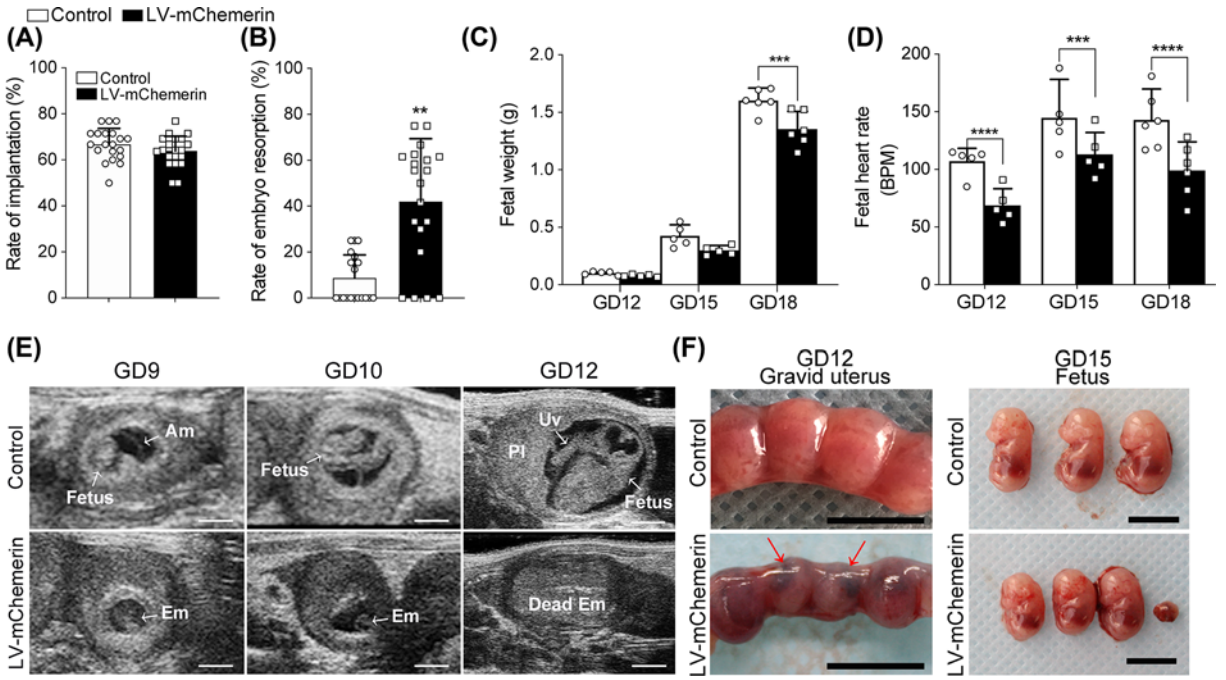


**Figure 3. Fetal characteristics in control mice and mice with trophoblast-specific chemerin overexpression**

(**A**,**B**) Rates of implantation and embryo resorption in control and LV-mChemerin mouse mothers (dead fetuses were excluded, mean ± SD of 20 mothers/group; $^{**}P<0.01$ by Student's *t* test (A) or Mann–Whitney U-test (B)). (**C**,**D**) Fetal weight and fetal heart rate (beats/min, BPM) at gestational days (GD) 12, 15 and 18 in control and LV-mChemerin mouse mothers (mean ± SD of $n\geq5$; $^{***}P<0.001$, $^{****}P<0.0001$ by two-way ANOVA with Sidak's multiple comparisons test). (**E**,**F**) Ultrasound imaging, gravid uterus and fetuses (scale bars representing 1, 10, and 5 mm, respectively, $n\geq5$) in the control and LV-mChemerin groups. Arrowheads in panel (F) illustrate hemorrhaging. Abbreviations: Am, amnion; Em, embryo; Pl, placenta; Uv, umbilical vein.

## Trophoblast-specific chemerin overexpression leads to increased pregnancy loss and fetal growth restriction

Although there was no difference in implantation rates between the control and LV-mChemerin groups (Figure 3A), the embryo resorption rate (including dead fetuses) was significantly increased in the LV-mChemerin group (Figure 3B). This suggests that chemerin does not affect blastocyst implantation. Both the fetal weight at GD18 (Figure 3C), and fetal heart rate at GD12, GD15, and GD18 (Figure 3D) were significantly reduced in the LV-mChemerin group. Placental weight was significantly reduced at GD12, GD15, but not at GD18 (Supplementary Figure S1G). Ultrasound imaging indicated that in the LV-mChemerin group, embryo development was delayed after GD9 and that some embryos stopped developing after GD10 and died (Figure 3E). The gross examination results of gravid uteri collected on GD12 showed focal hemorrhages at some of the implantation sites in the LV-mChemerin group (Figure 3F), and fetal growth restriction in the LV-mChemerin group on GD15 and GD18 (Figures 3F and Supplementary Figure S1A–C). Fetal weight correlated negatively with the serum chemerin levels at GD18 (Supplementary Figure S1D).

## Trophoblast-specific chemerin overexpression induces preeclampsia-like symptoms

Pregnancies with more than four fetuses surviving beyond GD15 in the LV-mChemerin group exhibited preeclampsia-like symptoms. Blood pressure was increased from GD15 to PD1, returning to control level at PD4 only (Figure 4A), while the urinary albumin/creatinine ratio was increased at GD18 (Figure 4B). H&E and PAS staining of the kidneys supported the presence of glomerular disorganization and endotheliosis (Figure 4C,D).

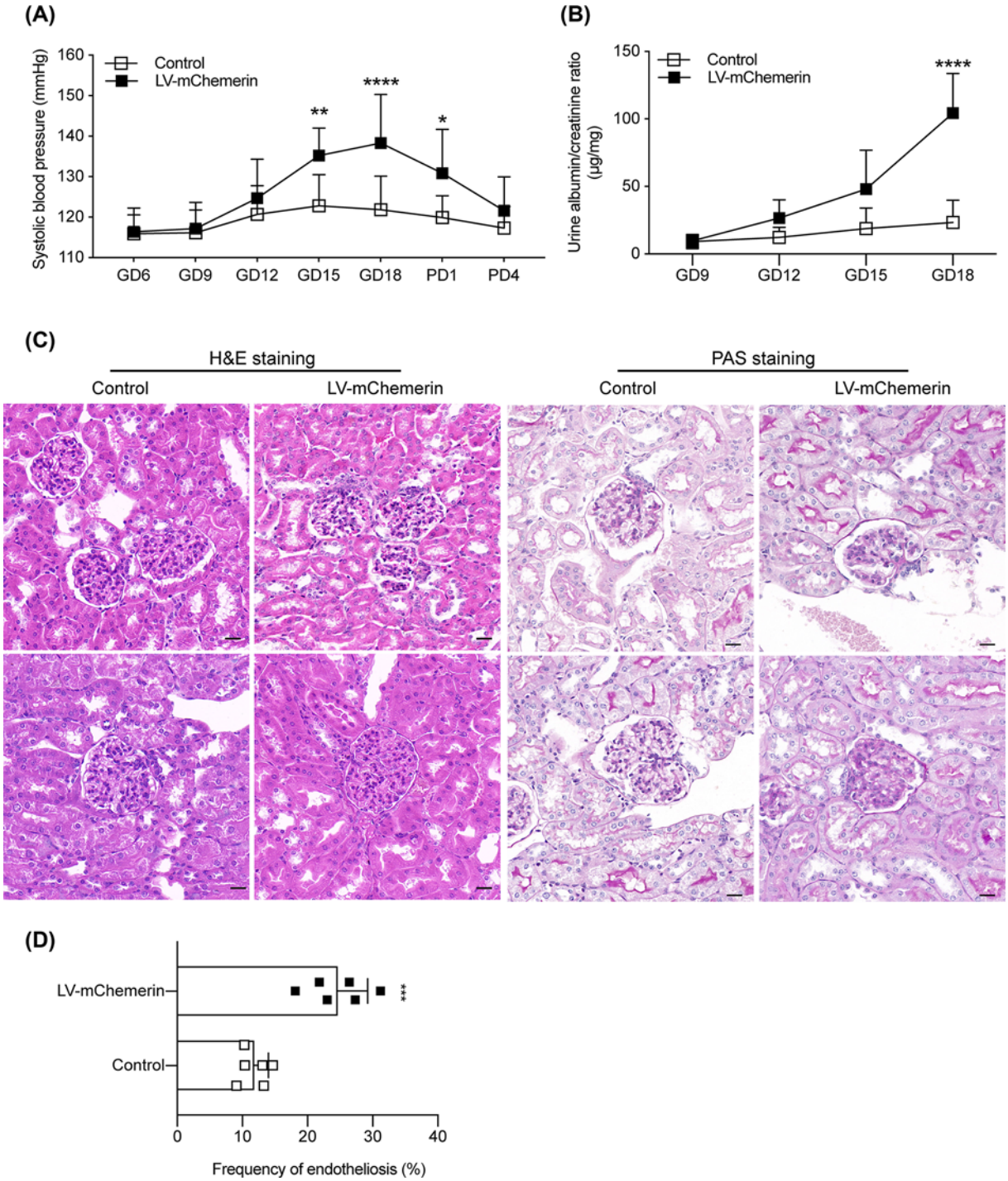


**Figure 4. Blood pressure, albumin excretion, and renal histology**

(**A**,**B**) SBP and urinary albumin/creatinine ratio in control and LV-mChemerin mouse mothers with more than four live fetuses at term on different gestational days (GDs). Data are mean ± SD of $n$=8; *$P$<0.05, **$P$<0.01, ****$P$<0.0001 by two-way ANOVA with Sidak's multiple comparisons test. (**C**) Representative H&E and PAS staining of kidney sections illustrating glomerular endotheliosis in the GD18 LV-mChemerin group (scale bar represents 25 μm; $n$≥5). (**D**) Glomerular endotheliosis on GD18 in the LV-mChemerin group versus control. Data are mean ± SD of $n$=6; ***$P$<0.001 by Student's $t$ test).

*Clinical Science* (2022) **136** 257–272
https://doi.org/10.1042/CS20210989

## Effects of trophoblast-specific chemerin overexpression on placental vasculature and trophoblasts

H&E staining of GD18 placentas showed disorganization in the junction zone and labyrinth layer in the LV-mChemerin group, while these were well-constructed in the control group (Figure 5A). Although labyrinth layer area was reduced in the LV-mChemerin mice, with a similar tendency for junction zone area (Figure 5C,D), their placental diameter and thickness were unaltered (Supplementary Figure S1E,F). ALP staining and CD31 IHC staining were used to locate trophoblasts and endothelial cells. This approach revealed that the cross-structures between these cells were disorganized in the LV-mChemerin mice (Figure 5B), while their labyrinth layer sinusoids area was reduced (Figure 5E). Moreover, cytokeratin 8 IHC staining indicated that there were fewer invasive trophoblasts around spiral arteries (Supplementary Figure S1H).

Cultured HTR8-Chemerin cells displayed elevated chemerin mRNA and protein levels (Supplementary Figure S2A–C) versus cultured HTR8-GFP control cells. CCRL2 expression was unchanged (Supplementary Figure S2B,C). During co-culture with HUVECs, branch length tended to be shorter ($P$=NS), while vessel-like tubes occurred less frequently when using HTR8-Chemerin cells (Supplementary Figure S2D–H). Importantly, when the CMKLR1 inhibitor α-NETA was added, the effects of chemerin overexpression were suppressed, and the HTR8-Chemerin/HUVEC co-culture resembled the HTR8 GFP/HUVEC co-culture.

## Trophoblastic chemerin overexpression leads to decreased expression of angiogenesis-related proteins through CMKLR1

In the chemerin-overexpressing placenta, CMKLR1 and CCRL2 mRNA and protein levels (Supplementary Figure S3A,B,E–G) were significantly increased at GD15 and GD18, while no differences were observed for both VEGF-A and sFlt-1 at the mRNA level (Supplementary Figure S3C,D). Analysis of molecules acting downstream of CMKLR1 showed significant decreases in the protein abundance of PI3K, Akt, and VEGF-A at GD15 and GD18, and of p-Akt at GD12 and GD18, while the protein abundance of sFlt-1 was increased at GD15 and GD18 ( Supplementary Figure S3E,H–L). The latter coincided with the elevated sFlt-1 and lowered PlGF levels in serum in the LV-mChemerin group (Supplementary Figure S4A,C), and both serum sFlt-1 and PlGF correlated significantly with the serum chemerin levels (Supplementary Figure S4B,D).

In HTR8-Chemerin cells, the CMKLR1 protein abundance was increased versus HTR8-GFP control cells (Supplementary Figure S5A,B). Similar to the changes in the chemerin-overexpressing placenta *in vivo*, PI3K, pAkt/Akt, and VEGF-A protein abundances were reduced, while sFlt-1 was increased in in HTR8-Chemerin cells (Supplementary Figure S5A,C–G). Treatment with α-NETA reversed the effects on PI3K, VEGF-A and sFlt-1 in HTR8-Chemerin cells.

Moreover, the rates of migration and invasion (Supplementary Figure S6A–D) by HTR8-Chemerin cells were reduced. Since MMP-2 and MMP-9 are likely players in trophoblast cell invasion [22], we quantified their protein expression. Reduced protein expression of MMP-2 but not MMP-9 was observed in HTR8-Chemerin cells (Supplementary Figure S6E–G). Here, α-NETA did not reverse these effects, and instead inhibited cell invasion in control cells (no statistical difference).

## Placental chemerin overexpression leads to increased expression of inflammation-related proteins

In the chemerin-overexpressing placenta, the protein levels of NFκB, TNF-α, and IL-1β were increased relative to those in control placentas at GD15 and GD18 (Figure 6A,B). Such elevations were also observed in HTR8-Chemerin cells versus HTR8-GFP control cells (Figure 6C,D), and α-NETA reversed this phenomenon.

Finally, serum ALT and AST levels at GD18 were unaltered in the LV-mChemerin group (Supplementary Figure S7A,B). Furthermore, hepatic chemerin levels increased during normal pregnancy, and fell back to pre-pregnancy levels at delivery day 7 (Supplementary Figure S7C). The latter drop was also observed in the LV-mChemerin group (Supplementary Figure S7D).

# Discussion

The present study is the first to show elevated expression and release of chemerin from human preeclamptic placentas, combined with a strong correlation between the circulating chemerin levels and the sFlt-1/PlGF ratio in pregnant women. In view of the fact that both circulating sFlt-1 and PlGF in pregnancy are largely placenta-derived [11], while their ratio is a well-known biomarker of preeclampsia severity [13], these data are supportive for the placenta as an

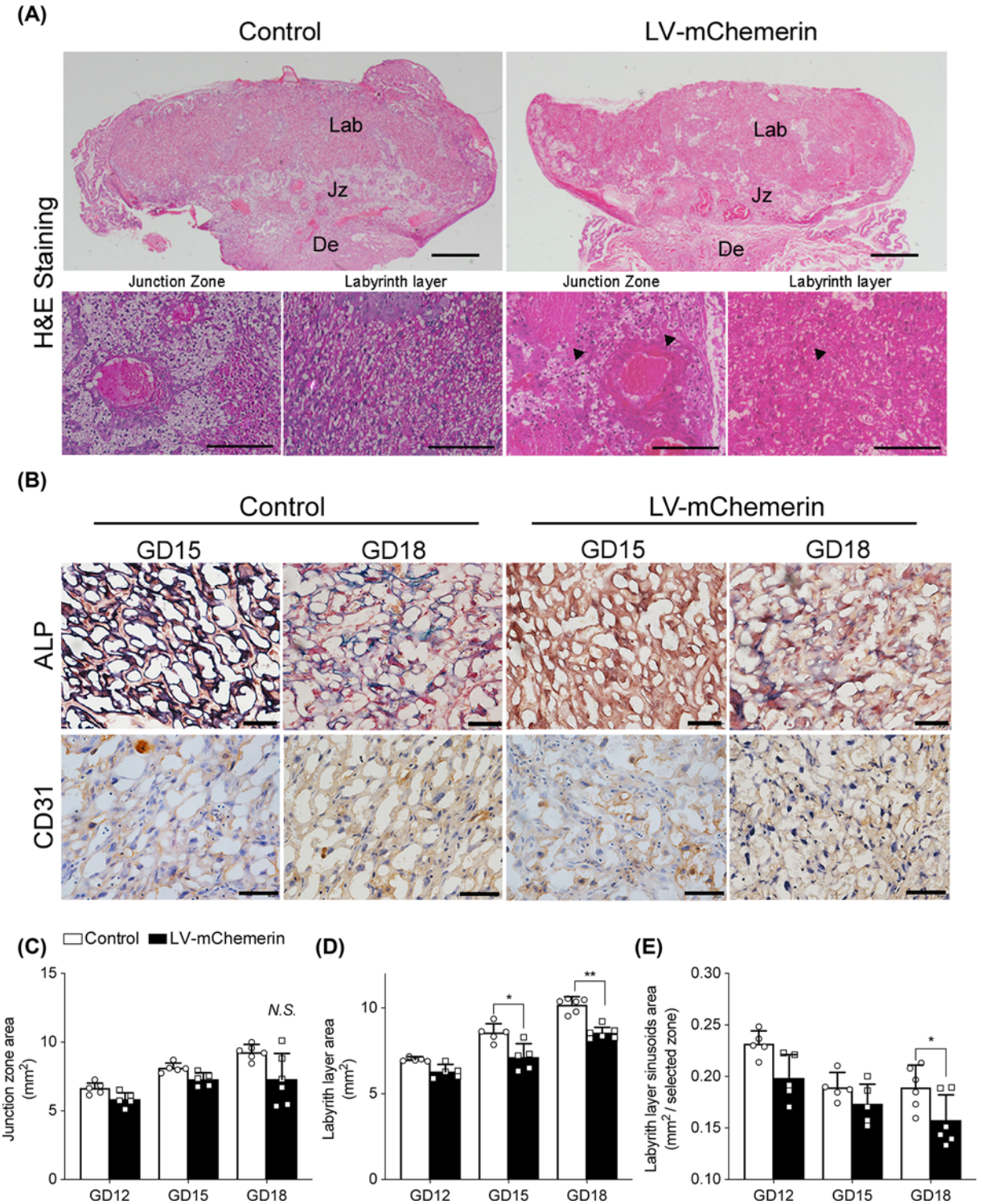


**Figure 5. Placental histology**

(**A**) Representative histology picture of placental sections from control and LV-mChemerin GD18 mouse mothers (scale bar represents 500 μm; $n \geq 5$). Black arrowheads point to congestion in veins at junction zone and disorganized structure of labyrinth vessels (scale bar represents 50 μm). (**B**) Placental ALP and CD31 staining on gestational day (GD) 12, 15, and 18 illustrating the disorganized cross-structure between trophoblast cells and vascular endothelial cells in the LV-mChemerin group (scale bar represents 100 μm; $n \geq 5$). (**C**–**E**) Quantification (on the basis of panels A,B) of junction zone area, labyrinth layer area, and the labyrinth layer sinusoids area. Data are mean ± SD of $n \geq 5$; $^{*}P < 0.05$, $^{**}P < 0.01$ by two-way ANOVA with Sidak's multiple comparisons test.

*Clinical Science* (2022) **136** 257–272
https://doi.org/10.1042/CS20210989

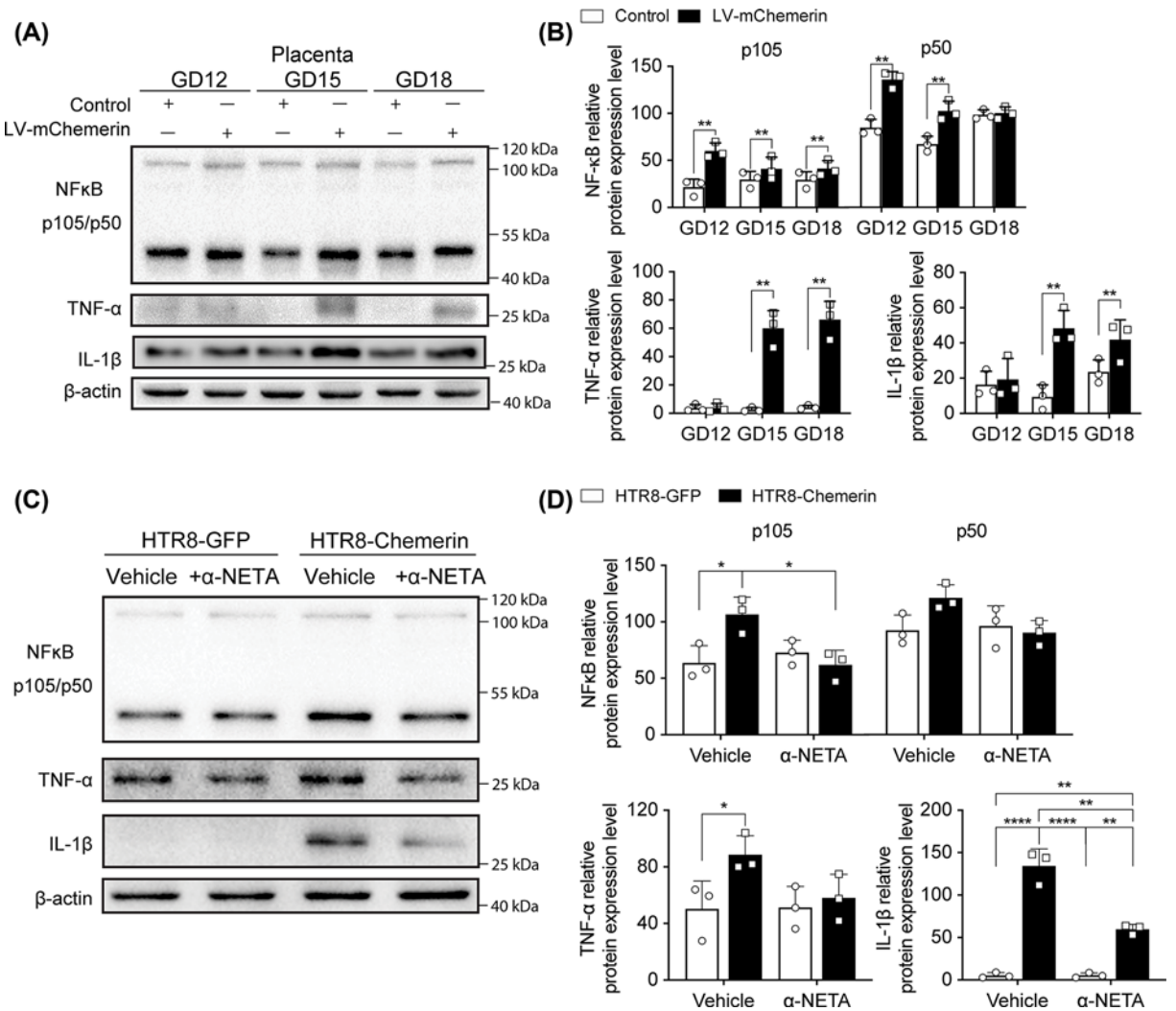


**Figure 6. Inflammatory proteins in placenta and cultured trophoblasts**

(**A**,**B**) NFκB p105/p50, TNF-α, and IL-1β at gestational day (GD) 12, 15, and 18 in control mice and chemerin-overexpressing (LV-mChemerin) mice measured by Western blotting, and expressed relative to β-actin. Data are mean ± SD of $n$=3; $^{**}P<0.01$ by two-way ANOVA with Sidak's multiple comparisons test. (**C**,**D**) NFκB p105/p50, TNF-α, and IL-1β in HTR8-GFP (Control) and HTR8-Chemerin (Chemerin) cells incubated in the absence (vehicle) or presence of 3 μmol/l α-NETA. Data are mean ± SD of $n$=3; $^{*}P<0.05$, $^{**}P<0.01$, $^{****}P<0.0001$ by two-way ANOVA with Sidak's multiple comparisons test.

important contributor to the elevated chemerin levels in preeclampsia. Moreover, trophoblast chemerin overexpression in pregnant mice was found to result in elevated circulating chemerin levels, and to induce a preeclampsia-like phenotype, characterized by diminished trophoblast invasion, a disorganized labyrinth layer, hypertension and proteinuria. *In-vitro* studies in chemerin-overexpressing HTR8/SVneo cells revealed that chemerin up-regulated inflammation-related proteins and sFlt-1 in a CMKLR1-dependent manner, thus diminishing migration and invasion, as well as tube formation during co-culturing with HUVECs. Taken together, these data suggest that placenta-derived chemerin disturbs normal placental development, is released into the circulation, and might act as a novel determinant of preeclampsia severity.

Under non-pregnant condition, adipose tissue and the liver are the main source of circulating chemerin [23]. The chemerin release from adipose tissue is unaltered in pregnancy [24]. In the present study, we observed an up-regulation of hepatic chemerin expression during pregnancy, which normalized after delivery. Most likely therefore, the rise in circulating chemerin during pregnancy is of both hepatic and placental origin, and only under preeclamptic conditions do levels occur that result in unwanted effects, in particular in the placenta. The rise in

circulating chemerin levels in control pregnant mice, which further increased in pregnant LV-mChemerin mice, supports a combined hepatic–placental origin. Notably, the rises in both serum and placental tissue chemerin levels became significant from GD15 only, although the placental chemerin mRNA levels were already elevated on GD12. This implies that before GD15 at most regional elevations of chemerin had occurred, which could not be detected when studying whole homogenates.

Placental disorganization, originating from impaired trophoblast invasion, is the main cause of preeclampsia [2]. This is due to the fact that trophoblast invasion underlies spiral artery remodeling in the maternal decidua and the establishment of maternal blood flow to the placenta. In the present study, cytokeratin 8 staining of the placenta revealed diminished trophoblast invasion in LV-mChemerin mice, while chemerin overexpression in HTR 8/SVneo cells led to impaired migration and invasion. Changes in chemerin expression also appeared to affect placenta formation and development. The murine labyrinth layer is a vasculature structure composed of fetal blood vessels and maternal blood sinuses separated by endothelia and layers of trophoblasts [25]. Adequate interaction of trophoblasts and endothelial cells in the first and second trimester is essential for a successful pregnancy, as it determines the placental microvascularization [26]. Overexpression of chemerin in trophoblasts was found to induce a disorganized structure in the labyrinth layer. Furthermore, when coculturing chemerin-overexpressing HTR 8/SVneo cells with HUVECs, tube formation was inhibited. Taken together, these data indicate that chemerin inhibits the interaction between trophoblast and endothelial cells, thus preventing normal placental development.

The PI3K/Akt signaling pathway, by stimulating MMPs, plays a key role in the regulation of trophoblast growth and invasion [22]. It is suppressed in preeclamptic placentas [27]. In human microvascular endothelial cells, chemerin has been reported to induce angiogenesis by up-regulating the PI3K/Akt-MMP pathway via its receptor CMKLR1 [28]. In our study, we observed up-regulation of both CMKLR1 and the non-signaling CCRL2 in the placenta of LV-mChemerin mice. CCRL2 may help to concentrate chemerin locally, allowing subsequent CMKLR1 stimulation [29]. Yet, despite CMKLR1 and CCRL2 up-regulation, we found that the placental PI3K/Akt-MMP-2 pathway was down-regulated, both *in vivo* in LV-mChemerin mice and *in vitro* in HTR8-Chemerin cells. Although this agrees with the observations in human preeclampsia, it opposes the findings in cultured human microvascular endothelial cells. An important caveat is that we measured protein expression, and not MMP activity. The CMKLR1 antagonist α-NETA did not reverse the effect on Akt and MMP-2 in chemerin-overexpressing cells, and even inhibited the invasion ability of control HTR8-GFP control cells. Since Yang et al. reported that intrauterine injection of α-NETA increased embryo resorption [30], CMKLR1 inhibition with this antagonist is unlikely to fully normalize the preeclampsia phenotype of our pregnant LV-mChemerin mice. Future studies should investigate how CMKLR1-CCRL2 interplay results in down-regulation of the PI3K/Akt-MMP pathway in our model.

Chemerin overexpression increased sFlt-1, and lowered VEGF-A and PlGF. This closely resembles the situation in human preeclampsia. Since α-NETA did reverse the VEGF-A and sFlt-1 alterations in HTR8-Chemerin cells, one possibility is that chemerin actually exerts its effects by up-regulating sFlt-1 via CMKLR1. Lowering sFlt-1 allows the return of the effects of VEGF-A on migration and invasion, in agreement with our observation that α-NETA restored the ability of tube formation when co-culturing chemerin-overexpressing HTR8/SVneo cells with HUVECs. Taken together, a likely scenario is that the chemerin/CMKLR1 pathway suppresses angiogenesis by increasing sFlt-1.

Up-regulation of inflammatory markers (e.g., NFκB, TNF-α, and IL-1β [31,32]) is a well-known phenomenon in preeclampsia. Chemerin induced an inflammatory response in multiple models [33,34]. In agreement with this view, in the present study chemerin overexpression also up-regulated NFκB, TNF-α, and IL-1β via CMKLR1, both in the mouse placenta and in cultured trophoblasts. To what degree these factors act locally, contributing to placental disorganization, or are released into the circulation, inducing systemic effects (including hypertension and proteinuria), remains to be determined. Given that chemerin levels are increased in hypertensive patients [35], while chemerin induces vasoconstriction CMKLR1 [35], chemerin itself might be responsible for the blood pressure rise in LV-mChemerin mice.

Spontaneous abortion in early pregnancy has been associated with low chemerin levels [30], although in PCOS patients the opposite was found [36]. We observed a negative correlation between the maternal chemerin levels and fetal weight in mice, while placental chemerin overexpression resulted in embryo resorption. These data imply that chemerin may play different roles at different stages of pregnancy, and that its levels should be within a specific range in a gestational age-dependent manner. Increased chemerin levels at the end of pregnancy may reflect excessive placental chemerin release, and could function as a novel determinant of preeclampsia severity, although its independency of the sFlt-1/PlGF ratio remains to be determined.

There are some limitations to our study. Firstly, we did not study the dose-dependency of trophoblast chemerin overexpression, nor do we know why chemerin would be elevated in preeclampsia at all. It may relate to the occurrence of dyslipidemia in this condition. Secondly, although such overexpression affected placental development, it remains

*Clinical Science* (2022) **136** 257–272
https://doi.org/10.1042/CS20210989

unclear how it induces preeclampsia-like symptoms in the mother. Thirdly, not only do we need to determine the contribution of the various chemerin receptors in the placenta and the rest of the body during pregnancy, but we should also unravel the relationship among chemerin, sFlt-1, and inflammation.

In conclusion, the placenta contributes to the elevated circulating chemerin level in PE, and placental trophoblast-specific overexpression of chemerin induces a preeclampsia-like syndrome in mice, characterized by severe placental vascular damage, intrauterine growth restriction, and embryonic lethality. Yet, whether inhibition of chemerin and its receptors is a novel therapeutic strategy for the clinical management of preeclampsia remains to be demonstrated.

## Clinical perspectives

- Preeclampsia is a major cause of maternal mortality, yet its pathogenesis remains unclear. Furthermore, maternal circulating levels of the adipokine chemerin are elevated in preeclampsia, but its origin and contribution to preeclampsia remain unknown.
- Placental chemerin expression and release were studied in human pregnancy, as well as the consequences of its overexpression in mice and trophoblasts. The human preeclamptic placenta released more chemerin. Placental overexpression of chemerin in mice yielded a preeclampsia-like syndrome, involving hypertension and proteinuria, combined with diminished trophoblast invasion, a disorganized labyrinth layer, and inflammation. In trophoblasts, elevated chemerin release inhibited migration and invasion, as well as tube formation during co-culture with endothelial cells.
- The preeclamptic placenta overexpresses chemerin and contributes to its elevated circulating levels in this condition. Interfering with chemerin might be a novel therapeutic option for the treatment of preeclampsia, while serum chemerin might be a new biomarker for the severity of this disease.

### Data Availability

All supporting data are available within the article and in the online-only Data Supplement.

### Competing Interests

The authors declare that there are no competing interests associated with the manuscript.

### Funding

This work was supported by the National Natural Science Foundation of China [grant numbers 81830041, 81771617, 81771611, 31572591]; the Shenzhen Basic Research Fund [grant numbers JCYJ20170413165233512, JCYJ20170412140326739]; the Guangdong Provincial Science and Technology Program [grant number 2019B030301009]; and the Shenzhen Key Laboratory of Metabolism and Cardiovascular Homeostasis [grant number ZDSYS20190902092903237].

### CRediT Author Contribution

**Lunbo Tan:** Data curation, Software, Formal analysis, Validation, Investigation, Visualization, Methodology, Writing—original draft, Writing—review & editing. **Zhilong Chen:** Data curation, Software, Formal analysis, Validation, Investigation, Visualization, Writing—original draft, Writing—review & editing. **Fen Sun:** Data curation, Formal analysis, Validation, Investigation, Visualization, Writing—original draft, Writing—review & editing. **Zhuoqun Zhou:** Resources, Data curation, Formal analysis, Investigation, Writing—original draft, Writing—review & editing. **Baozhen Zhang:** Data curation, Formal analysis, Visualization, Writing—original draft, Writing—review & editing. **Baobei Wang:** Data curation, Formal analysis, Validation, Visualization, Writing—original draft, Writing—review & editing. **Jie Chen:** Resources, Software, Validation, Writing—original draft, Writing—review & editing. **Mengxia Li:** Resources, Software, Formal analysis, Validation, Writing—original draft, Writing—review & editing. **Tianxia Xiao:** Resources, Software, Writing—original draft, Project administration, Writing—review & editing. **Rugina I. Neuman:** Data curation, Formal analysis, Validation, Writing—original draft, Writing—review & editing. **Jianmin Niu:** Resources, Funding acquisition, Writing—original draft, Writing—review & editing. **Koen Verdonk:** Resources, Supervision, Validation, Writing—original draft, Writing—review & editing. **Xifeng Lu:** Resources, Supervision, Funding acquisition, Writing—original draft, Writing—review & editing. **Jian V. Zhang:** Resources, Supervision, Funding acquisition, Methodology, Writing—original draft, Project administration,

Writing—review & editing. **A.H. Jan Danser:** Resources, Supervision, Validation, Investigation, Writing—original draft, Project administration, Writing—review & editing. **Qing Yang:** Conceptualization, Resources, Supervision, Funding acquisition, Validation, Investigation, Methodology, Writing—original draft, Writing—review & editing. **Xiujun Fan:** Conceptualization, Resources, Supervision, Funding acquisition, Methodology, Writing—original draft, Project administration, Writing—review & editing.

## Acknowledgements

The authors would like to thank Fei Yan at the Paul C. Lauterbur Research Center for Biomedical Imaging of SIAT for the provision of ultrasound machines.

## Abbreviations

α-NETA, 2-(α-naphthoyl)ethyl trimethylammonium iodide; ALP, alkaline phosphatase; CCRL2, CC motif chemokine receptor-like 2; CMKLR1 or ChemR23, chemokine-like receptor 1; DBP, diastolic blood pressure; FBS, fetal bovine serum; HUVEC, human umbilical vein endothelial cell; H&E, Hematoxylin and Eosin; IHC, immunohistochemical; IL, interleukin; ISSHP, International Society for the Study of Hypertension in Pregnancy; MMP, matrix metalloproteinase; NFκB, nuclear factor-κB; PAS, Periodic acid–Schiff; PFA, paraformaldehyde; PlGF, placental growth factor; SBP, systolic blood pressure; sFlt-1, soluble Fms-like tyrosine kinase-1; TNF, tumor necrosis factor; VEGF, vascular endothelial growth factor.

# References

1 Ilekis, J.V., Reddy, U.M. and Roberts, J.M. (2007) Preeclampsia–a pressing problem: an executive summary of a National Institute of Child Health and Human Development workshop. *Reprod. Sci.* **14**, 508–523, https://doi.org/10.1177/1933719107306232
2 Steegers, E.A., von Dadelszen, P., Duvekot, J.J. and Pijnenborg, R. (2010) Pre-eclampsia. *Lancet* **376**, 631–644, https://doi.org/10.1016/S0140-6736(10)60279-6
3 Garces, M.F., Sanchez, E., Acosta, B.J., Angel, E., Ruiz, A.I., Rubio-Romero, J.A. et al. (2012) Expression and regulation of chemerin during rat pregnancy. *Placenta* **33**, 373–378, https://doi.org/10.1016/j.placenta.2012.02.007
4 Carlino, C., Trotta, E., Stabile, H., Morrone, S., Bulla, R., Soriani, A. et al. (2012) Chemerin regulates NK cell accumulation and endothelial cell morphogenesis in the decidua during early pregnancy. *J. Clin. Endocrinol. Metab.* **97**, 3603–3612, https://doi.org/10.1210/jc.2012-1102
5 Rourke, J.L., Dranse, H.J. and Sinal, C.J. (2013) Towards an integrative approach to understanding the role of chemerin in human health and disease. *Obes. Rev.* **14**, 245–262, https://doi.org/10.1111/obr.12009
6 Garces, M.F., Sanchez, E., Ruiz-Parra, A.I., Rubio-Romero, J.A., Angel-Muller, E., Suarez, M.A. et al. (2013) Serum chemerin levels during normal human pregnancy. *Peptides* **42**, 138–143, https://doi.org/10.1016/j.peptides.2013.01.003
7 Yang, X., Quan, X., Lan, Y., Ye, J., Wei, Q., Yin, X. et al. (2017) Serum chemerin level during the first trimester of pregnancy and the risk of gestational diabetes mellitus. *Gynecol. Endocrinol.* **33**, 770–773, https://doi.org/10.1080/09513590.2017.1320382
8 Cetin, O., Kurdoglu, Z., Kurdoglu, M. and Sahin, H.G. (2017) Chemerin level in pregnancies complicated by preeclampsia and its relation with disease severity and neonatal outcomes. *J. Obstet. Gynaecol.* **37**, 195–199
9 Xu, Q.L., Zhu, M., Jin, Y., Wang, N., Xu, H.X., Quan, L.M. et al. (2014) The predictive value of the first-trimester maternal serum chemerin level for pre-eclampsia. *Peptides* **62**, 150–154, https://doi.org/10.1016/j.peptides.2014.10.002
10 Smolinska, N., Kiezun, M., Dobrzyn, K., Rytelewska, E., Kisielewska, K., Gudelska, M. et al. (2019) Expression of chemerin and its receptors in the porcine hypothalamus and plasma chemerin levels during the oestrous cycle and early pregnancy. *Int. J. Mol. Sci.* **20**, 3887, https://doi.org/10.3390/ijms20163887
11 Saleh, L., van den Meiracker, A.H., Geensen, R., Kaya, A., Roeters van Lennep, J.E., Duvekot, J.J. et al. (2018) Soluble fms-like tyrosine kinase-1 and placental growth factor kinetics during and after pregnancy in women with suspected or confirmed pre-eclampsia. *Ultrasound Obstet. Gynecol.* **51**, 751–757, https://doi.org/10.1002/uog.17547
12 Brown, M.A., Magee, L.A., Kenny, L.C., Karumanchi, S.A., McCarthy, F.P., Saito, S. et al. (2018) Hypertensive disorders of pregnancy: ISSHP Classification, Diagnosis, and Management Recommendations for International Practice. *Hypertension* **72**, 24–43, https://doi.org/10.1161/HYPERTENSIONAHA.117.10803
13 Saleh, L., Vergouwe, Y., van den Meiracker, A.H., Verdonk, K., Russcher, H., Bremer, H.A. et al. (2017) Angiogenic markers predict pregnancy complications and prolongation in preeclampsia: continuous versus cutoff values. *Hypertension* **70**, 1025–1033, https://doi.org/10.1161/HYPERTENSIONAHA.117.09913
14 Hitzerd, E., Broekhuizen, M., Mirabito Colafella, K.M., Glisic, M., de Vries, R., Koch, B.C.P. et al. (2019) Placental effects and transfer of sildenafil in healthy and preeclamptic conditions. *EBioMedicine* **45**, 447–455, https://doi.org/10.1016/j.ebiom.2019.06.007
15 Hitzerd, E., Neuman, R.I., Broekhuizen, M., Simons, S.H.P., Schoenmakers, S., Reiss, I.K.M. et al. (2020) Transfer and vascular effect of endothelin receptor antagonists in the human placenta. *Hypertension* **75**, 877–884, https://doi.org/10.1161/HYPERTENSIONAHA.119.14183
16 Neuman, R.I., Alblas van der Meer, M.M., Nieboer, D., Saleh, L., Verdonk, K., Kalra, B. et al. (2020) PAPP-A2 and Inhibin A as novel predictors for pregnancy complications in women with suspected or confirmed preeclampsia. *J. Am. Heart Assoc.* **9**, e018219, https://doi.org/10.1161/JAHA.120.018219
17 Fan, X., Rai, A., Kambham, N., Sung, J.F., Singh, N., Petitt, M. et al. (2014) Endometrial VEGF induces placental sFLT1 and leads to pregnancy complications. *J. Clin. Invest.* **124**, 4941–4952, https://doi.org/10.1172/JCI76864

*Clinical Science* (2022) **136** 257–272
https://doi.org/10.1042/CS20210989

18 Fan, X., Ren, P., Dhal, S., Bejerano, G., Goodman, S.B., Druzin, M.L. et al. (2011) Noninvasive monitoring of placenta-specific transgene expression by bioluminescence imaging. *PLoS ONE* **6**, e16348, https://doi.org/10.1371/journal.pone.0016348
19 Zhang, B., Tan, L., Yu, Y., Wang, B., Chen, Z., Han, J. et al. (2018) Placenta-specific drug delivery by trophoblast-targeted nanoparticles in mice. *Theranostics* **8**, 2765–2781, https://doi.org/10.7150/thno.22904
20 Xiao, Z., Li, S., Yu, Y., Li, M., Chen, J., Wang, F. et al. (2018) VEGF-A regulates sFlt-1 production in trophoblasts through both Flt-1 and KDR receptors. *Mol. Cell. Biochem.* **449**, 1–8, https://doi.org/10.1007/s11010-018-3337-5
21 Aldo, P.B., Krikun, G., Visintin, I., Lockwood, C., Romero, R. and Mor, G. (2007) A novel three-dimensional in vitro system to study trophoblast-endothelium cell interactions. *Am. J. Reprod. Immunol.* **58**, 98–110, https://doi.org/10.1111/j.1600-0897.2007.00493.x
22 Cohen, M., Meisser, A. and Bischof, P. (2006) Metalloproteinases and human placental invasiveness. *Placenta* **27**, 783–793, https://doi.org/10.1016/j.placenta.2005.08.006
23 Bozaoglu, K., Bolton, K., McMillan, J., Zimmet, P., Jowett, J., Collier, G. et al. (2007) Chemerin is a novel adipokine associated with obesity and metabolic syndrome. *Endocrinology* **148**, 4687–4694, https://doi.org/10.1210/en.2007-0175
24 Sanchez-Rebordelo, E., Cunarro, J., Perez-Sieira, S., Seoane, L.M., Dieguez, C., Nogueiras, R. et al. (2018) Regulation of chemerin and CMKLR1 expression by nutritional status, postnatal development, and gender. *Int. J. Mol. Sci.* **19**, 2905, https://doi.org/10.3390/ijms19102905
25 Schreiber, J., Riethmacher-Sonnenberg, E., Riethmacher, D., Tuerk, E.E., Enderich, J., Bosl, M.R. et al. (2000) Placental failure in mice lacking the mammalian homolog of glial cells missing, GCMa. *Mol. Cell. Biol.* **20**, 2466–2474, https://doi.org/10.1128/MCB.20.7.2466-2474.2000
26 Wang, Y. and Zhao, S. (2010) *Vascular Biology of the Placenta*, San Rafael (CA)
27 Xu, Y., Sui, L., Qiu, B., Yin, X., Liu, J. and Zhang, X. (2019) ANXA4 promotes trophoblast invasion via the PI3K/Akt/eNOS pathway in preeclampsia. *Am. J. Physiol. Cell Physiol.* **316**, C481–C491, https://doi.org/10.1152/ajpcell.00404.2018
28 Kaur, J., Adya, R., Tan, B.K., Chen, J. and Randeva, H.S. (2010) Identification of chemerin receptor (ChemR23) in human endothelial cells: chemerin-induced endothelial angiogenesis. *Biochem. Biophys. Res. Commun.* **391**, 1762–1768, https://doi.org/10.1016/j.bbrc.2009.12.150
29 Mattern, A., Zellmann, T. and Beck-Sickinger, A.G. (2014) Processing, signaling, and physiological function of chemerin. *IUBMB Life* **66**, 19–26, https://doi.org/10.1002/iub.1242
30 Yang, X., Yao, J., Wei, Q., Ye, J., Yin, X., Quan, X. et al. (2018) Role of chemerin/CMKLR1 in the maintenance of early pregnancy. *Front. Med.* **12**, 525–532, https://doi.org/10.1007/s11684-017-0577-9
31 Freeman, D.J., McManus, F., Brown, E.A., Cherry, L., Norrie, J., Ramsay, J.E. et al. (2004) Short- and long-term changes in plasma inflammatory markers associated with preeclampsia. *Hypertension* **44**, 708–714, https://doi.org/10.1161/01.HYP.0000143849.67254.ca
32 Vaughan, J.E. and Walsh, S.W. (2012) Activation of NF-kappaB in placentas of women with preeclampsia. *Hypertens. Pregnancy* **31**, 243–251, https://doi.org/10.3109/10641955.2011.642436
33 Herenius, M.M., Oliveira, A.S., Wijbrandts, C.A., Gerlag, D.M., Tak, P.P. and Lebre, M.C. (2013) Anti-TNF therapy reduces serum levels of chemerin in rheumatoid arthritis: a new mechanism by which anti-TNF might reduce inflammation. *PLoS ONE* **8**, e57802, https://doi.org/10.1371/journal.pone.0057802
34 Berg, V., Sveinbjornsson, B., Bendiksen, S., Brox, J., Meknas, K. and Figenschau, Y. (2010) Human articular chondrocytes express ChemR23 and chemerin; ChemR23 promotes inflammatory signalling upon binding the ligand chemerin(21-157). *Arthritis Res. Ther.* **12**, R228, https://doi.org/10.1186/ar3215
35 Yang, M., Yang, G., Dong, J., Liu, Y., Zong, H., Liu, H. et al. (2010) Elevated plasma levels of chemerin in newly diagnosed type 2 diabetes mellitus with hypertension. *J. Investig. Med.* **58**, 883–886, https://doi.org/10.2310/JIM.0b013e3181ec5db2
36 Yang, X., Quan, X., Lan, Y., Wei, Q., Ye, J., Yin, X. et al. (2018) Serum chemerin level in women with PCOS and its relation with the risk of spontaneous abortion. *Gynecol. Endocrinol.* **34**, 864–867, https://doi.org/10.1080/09513590.2018.1462316